International Journal of Multiphase Flow 34 (2008) 950–965

Contents lists available at ScienceDirect

International Journal of Multiphase Flow

journal homepage: www.elsevier.com/locate/ijmulflow

Experimental validation of theoretical models in two-phase high-viscosity ratio liquid–liquid flows in horizontal and slightly inclined pipes

B. Grassi *, D. Strazza, P. Poesio

Università degli Studi di Brescia, Via Branze 38, 25123 Brescia, Italy

ARTICLE INFO

Article history:
Received 27 September 2007
Received in revised form 19 March 2008
Available online 11 April 2008

Keywords:
Oil–water
High-viscosity oil
Flow pattern
Pressure drop

ABSTRACT

Liquid–liquid flow literature proposes models developed to predict quantities and phenomena of interest, once given fluid properties and the features of the flow domain. The validity of any model should be verified through experimental observations, being this practice an effective way to evaluate the model conditions of applicability and possible limitations. Despite the fact that several works have already been proposed on the validation of theoretical models, most of them concern liquids characterised by low viscosity ratio $\tilde{\mu}$, while in industrial realities (such as petroleum or food ones) the liquids involved are often characterised by high viscosity ratios. The extension of low-$\tilde{\mu}$ results to high-$\tilde{\mu}$ flows is not straightforward, so that it is necessary to validate the models for the latter case specifically. This work presents experimental pressure drops and flow-pattern maps associated to the flow of oil and water in horizontal and slightly inclined pipe, where the chosen liquids are characterised by an oil-to-water viscosity ratio of about 800:1 at 20 °C. Various theoretical models have been considered, with particular attention to core-annular flow two-fluid model and oil-in-water dispersion homogeneous no-slip model for the prediction of associated pressure drops, and flow-pattern map transition criteria involving the regimes encountered in the experimental tests. The theoretical predictions have been then compared to the experimental results. A satisfactory agreement has been found especially as concerns pressure drop comparisons. As regards the predicted transition boundaries superimposed on the corresponding flow-pattern maps, the 'free' parameters have been fitted on the basis of experimental results and observations, and the final agreement is good in the prediction of both the core-annular flow region of existence and the transition to oil-in-water dispersion. No conclusion can be expressed on transition criteria involving stratified flow, which only seldom has been observed in the performed experiments.

1. Introduction

Liquid–liquid flows represent a subcategory of multiphase flows that has been rising growing interest since the second half of the 20th Century. On the one side, the knowledge of the driving mechanisms at the base of the simultaneous flow of two liquid phases in a domain cannot be considered acquired. On the other side, however, experimental and theoretical investigations indicate that such mechanisms cannot be entirely borrowed from gas–liquid field, for which a wider literature is already available at the present time. Besides rising a purely scientific interest, liquid–liquid flows represent also an attractive topic from the industrial viewpoint, due to the growing need for optimisation and control.

Various experimental works have been proposed in the literature to enhance the understanding of liquid–liquid flows – some of which had the general purpose of creating a database of experiments to explore how two liquids of given properties behave when flowing together in a given domain. The first documented experimental investigations on liquid–liquid flows date back to the late 1950s. The works by Russell et al. (1959), who performed a systematic series of experiments on oil–water flows and contextually proposed a first classification of the observed flow-patterns, Russell and Charles (1959) and Charles et al. (1961), not only established the basis for the study of liquid–liquid flows, but represented also the main resource of data for many years to come. Indeed, it was only ten years later that new consistent experimental studies on flow-patterns and pressure drops were performed by Guzhov and Medvedev (1971) and Guzhov et al. (1973). Such early works proved definitively the inadequacy of gas–liquid models to predict the behaviour of liquid–liquid flows, actually opening a new way.

Most of the following works focused on a single flow regime in order to individuate the fundamental mechanisms underlying its behaviour, or its practical implications from the viewpoint of its application in industry. Experimental works on stratified flow are reported in Trallero (1995), Lovick and Angeli (2004) and Sunder Raj et al. (2005). Arirachakaran et al. (1989), Nädler and Mewes

* Corresponding author. Tel.: +39 0303715494; fax: +39 0303702448.
E-mail address: benedetta.grassi@ing.unibs.it (B. Grassi).

0301-9322/$ - see front matter © 2008 Elsevier Ltd. All rights reserved.
doi:10.1016/j.ijmultiphaseflow.2008.03.006

(1997) and Angeli and Hewitt (1998) performed experiments with oil and water dispersions and emulsions, and focused their attention on the complex phenomenon of phase inversion – see also Ioannou et al. (2005), Hu et al. (2006) and Piela et al. (2006). As concerns core-annular flow experimental studies, Russell and Charles (1959), Hasson et al. (1970), Arney et al. (1992), Bannwart (1998), Sotgia and Tartarini (2004) and Strazza et al. (2007) can be cited as significant examples. Only few publications can be found instead on liquid–liquid slug flow – see Zhao et al. (2006) and Poesio et al. (2007).

Besides the experimental investigation, another tool to study liquid–liquid flows is the theoretical (or semiempirical) modelling. Typical examples are flow regime-dependent models which allow to predict pressure drop and phase hold-up, once given input flow-rates, fluid properties and set-up geometry, but recent works deal also with the so-called 'inverse' modelling, consisting of computing liquid flow-rates based on pressure drop and hold-up measurements (Hadžiabdić and Oliemans, 2007). To overcome the limitations imposed by a flow regime-dependent approach, criteria have also been proposed to build theoretical flow-pattern maps once known fluid physical properties and set-up features, generally based on stability analyses or empirical considerations (Brauner and Moalem Maron, 1992).

Clearly, the validity of any model should be properly checked via experimental observations. Though remarkable work has been done to this purpose, most experimental validations have been performed with liquids characterised by low viscosity ratios – see, for instance, Trallero (1995), Sunder Raj et al. (2005), and Rodriguez and Oliemans (2006) – while very few can be found in the literature on liquid–liquid flows characterised by high viscosity ratio, despite the fact that the latter case can be so frequently encountered in the industrial experience (e.g.: petroleum and food industry). Since it is expected that liquid–liquid flow behaviour strongly depends on the viscosity ratio, in a way which cannot be predicted *a priori*, it proves necessary to investigate the validity of the models in such a distinct situation.

The aim of the present work is to give a contribution in this direction, as the possibility to make accurate prediction on quantities and phenomena of interest would be an important achievement from the scientific viewpoint and a powerful tool from the industrial one. In the light of a series of experimental tests performed at the University of Brescia, the validity of models developed and summarised by Brauner (2002) for the prediction of pressure drops in core-annular and oil-in-water dispersed flows, and for the prediction of flow regime regions in the flow-pattern map, will be analysed. The two liquids chosen for the experimental campaigns are paraffin oil and tap water which are characterised by an oil-to-water viscosity ratio of about 800:1 at 20 °C.

Section 2 describes the experimental set-up used for the tests and shows the most significant results in terms of flow-pattern maps and pressure drops. In Section 3, the predictions by Brauner (2002) predictions in terms of pressure drops and flow-pattern transitions are superimposed to the experimental data in order to examine the effectiveness of the models and to give a contribution in the direction of their validation. Finally, Section 4 summarises the conclusions of the study. Appendix A reports a discussion on the choices operated by various authors concerning the problem of where to place the measurement section if comparisons to fully-developed-flow model predictions have to be performed.

2. Experiments

The experimental facility in which all the tests and measurements have been performed has been built at the University of Brescia. A schematic of the facility is shown in Fig. 1. The experimental set-up has been built to simulate the flow of two immiscible liquids within a pipe. The fluids used are oil and water, whose physical properties are reported in Table 1, which are initially stored in two different 1 m^3 tanks.

A water pump and an oil pump move the two fluids from the respective storage tanks to the test section. The two fluids are then

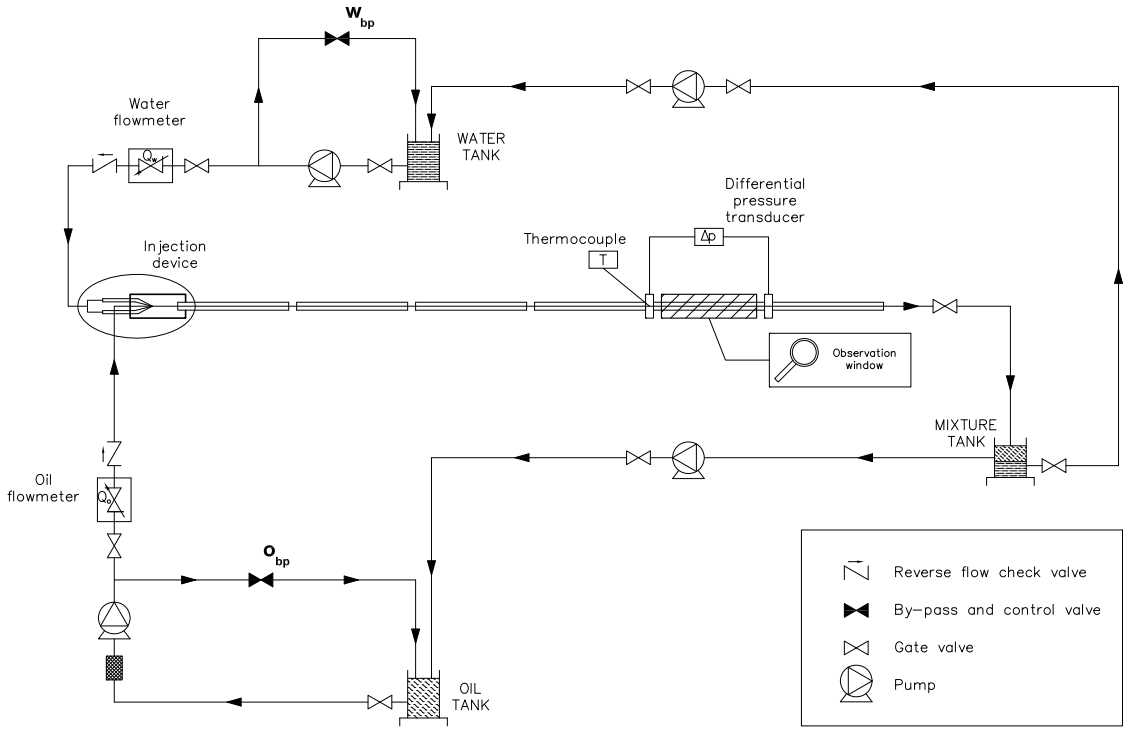

Fig. 1. Schematic of the experimental facility.

Table 1
Physical properties of raw fluids

Oil	Water
$\rho_o = 886\ kg\ m^{-3}$	$\rho_w = 1000\ kg\ m^{-3}$
$\mu_o\ (20\ ^\circ C) = 0.799\ Pa\ s$	$\mu_w = 0.0013\ Pa\ s$
$\mu_o\ (25\ ^\circ C) = 0.653\ Pa\ s$	
$\mu_o\ (30\ ^\circ C) = 0.533\ Pas$	
$\sigma = 0.05\ N\ m^{-1}$	

sent into an injection device (whose features are described later in this section) that controls their introduction into the pipe. Before entering the device, oil flow-rate is measured by a screw-spindle flow-meter while water flow-rate is measured by a rotating vane flow-meter (actually, one for high water flow-rates and one for low water flow-rates to keep the experimental uncertainty as lowest as possible over the entire range).

The test pipe consists of six transparent polycarbonate tubes of 21 mm internal diameter, leading to a total 9 m long pipe. The pipe is sustained by a steel beam, which is hinged midway to a vertical 1.2 m high support. The beam rotation around such hinge allows the system inclination up to $\pm 15^\circ$. The test section is placed at the 5th tube, so that a 6 m upstream and a 1.5 m downstream lengths separate it from the inlet and the outlet, respectively. A glass box filled with water is placed midway the test section, see Fig. 1, in order to correct the optical distortions induced by pipe wall curvature and to allow easy observations and camera recording. Two aluminium pressure ports are inserted on-line at the edges of the same measurement section. The plugs are connected via PVC pipes to the differential pressure transducer which measures the frictional pressure differential between them – that is, on a 1.5 m tract. Besides, in the high-pressure plug a thermocouple is inserted into a thin hole to monitor the thermal condition of the flow.

Oil-and-water mixture flows through the pipe and is then collected in a 1 m^3 tank, where the two fluids separate as a consequence of density difference. Once separated, oil occupies the upper part of the collection tank and water fills the lower layer. The two fluids can then be pumped back to their respective storage tanks.

By means of the described experimental facility, the simultaneous flow of oil and water in the pipe has been studied in case of horizontal, upward-inclined and downward-inclined system, in terms of flow-pattern maps and pressure drops. Thus, each experimental point consists of three measurements: water flow-rate, oil flow-rate and pressure drop on a 1.5 m length. At the same time, a visual observation of the established flow-pattern is associated to each measurement array.

The choice of the mixing device is an important step in test planning. In particular, it was observed that inserting the liquids into the pipe already in the core-annular configuration is a favourable condition to the onset of core-annular flow through the tube (Brauner, 1998). Indeed, Grassi et al. (2006) reported dramatic changes in the flow-pattern maps obtained in the same experimental set-up with different devices, and, from the comparison among four different devices, the one represented in Fig. 2 appeared to be the most suitable to promote core-annular flow; choosing a device with an axial oil injection and a 'punch-like' water injection, instead, resulted in the vanishing of core-annular and slug flow regimes. For the purposes of the present paper, the device of Fig. 2 was chosen. It can be seen that water is injected into an inner chamber of the device through four holes spaced apart 90° along a circumference on the device cover, while oil is pumped into a plexiglass tube. As can be seen in Fig. 2, the last 50 mm of the plexiglass tube stick out of the chamber and end up in the test pipe, which is flanged directly to the inlet device. Along these 50 mm, water is still constrained between two solid surfaces (test pipe internal wall and plexiglass tube external wall), until the plexiglass tube is over and water finally meets the oil.

Flow-pattern maps – Fig. 3 shows the experimental flow-pattern maps obtained in case of horizontal oil–water flow, while in Fig. 4a–c the results obtained for inclined pipes are reported. As it can be seen from the comparison among the maps, no substantial differences are induced by slight variation of the pipe inclination angle, thus the following analysis applies to all the proposed results. All the maps show that core-annular and oil-in-water dispersion regimes have been obtained in a wide range of input flow-rates, while slug flow can be seen in relatively small portions of the flow map, and stratified flow-patterns have rarely been observed, due to technical limitations of the pumping system. In order to give an interpretation of these results, it can be recalled that Brauner (2002) stressed the importance of the Eötvös number, defined as

$$Eo = \frac{(\rho_w - \rho_o) g D^2}{8\sigma} \tag{1}$$

as a characterising parameter of a system, where D, ρ_w, ρ_o, σ and g represent internal diameter of the pipe, water and oil densities, superficial tension between the two fluids and gravity acceleration, respectively. It was noted that low Eo and high Eo systems exhibit very different behaviour in terms of flow-pattern maps, transition boundaries and regime occurrences. The characteristic Eötvös number of the system described in the present work is $Eo \sim 1.2$. In the light of Brauner (2002) considerations, the intermediate value of the Eötvös number characterising the set-up can be thought as the origin of a 'hybrid' system behaviour. In particular, under the conditions described above, the core-annular regime can be

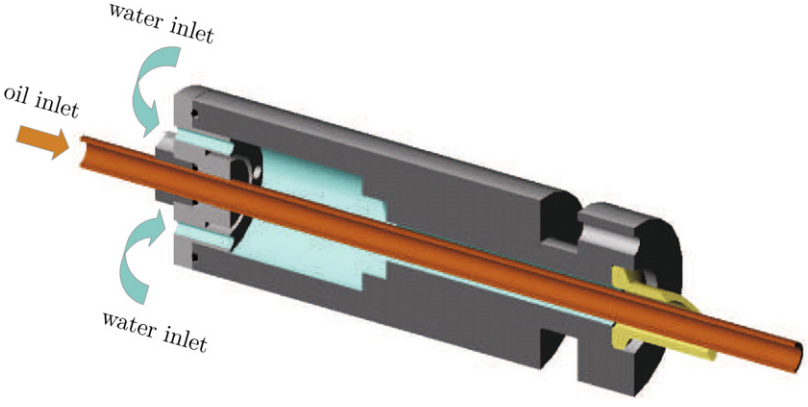

Fig. 2. The injection device.

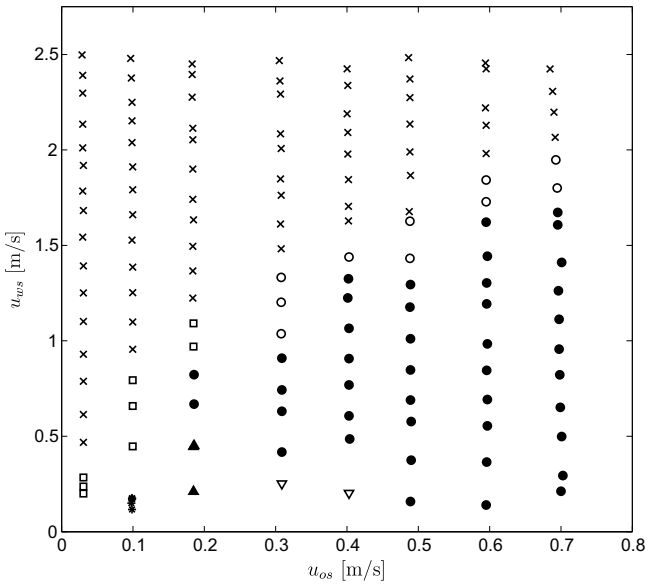

Fig. 3. Experimental flow-pattern map (0°). u_{ws}, u_{os}: water and oil superficial velocities. ▲ = *stratified flow*; × = *dispersion of oil in water*; • = *core-annular flow*; □ = *plug/slug flow*; ▽ = *stratified flow and dispersion of oil in water*; ○ = *core-annular flow and oil in water dispersion*; ∗ = *oil film at the wall and inner dispersion of oil in water*.

obtained for oil superficial velocities ranging from 0.2 m/s to the maximum achieved 0.7 m/s velocity. Examples of observed core-annular flows are shown in Fig. 5.

The observed dispersion range from very dilute oil-in-water dispersions to more concentrated dispersions of larger oil drops; some examples have been reported in Fig. 6. Water-in-oil dispersions have never been observed in any experimental test. Slug flow appears at very low oil flow-rates when water superficial velocity is low enough to avoid fragmentation of drops due to inertia forces, and at the same time it is high enough to avoid oil fouling. Fig. 7 shows pictures of slug flow, intended as the alternation of elongated drops and water cells. It is to be noted that the elongated drops observed in the present work are always separated from the pipe wall by a film of water.

Pressure drops – Pressure measurements are reported in Fig. 8 for horizontal system, and in Fig. 9a–c as regards inclined systems. Here the measured pressure gradients are reported as a function of the input water fraction: different symbols indicate different observed flow regimes, and different colours represent different oil flow-rates. From the analysis, it is evident that core-annular flows are generally obtained with the highest oil flow-rates explored and for low water input fraction. The trend line of each iso-u_{os} set of data shows that core-annular flow points correspond to pressure gradient comparable to the pressure gradient associated to the single-phase flow of water alone in the same pipe at the mixture velocity – see Fig. 10.

Oil-in-water dispersed flows, on the contrary, are achieved through high water input fractions and for the lowest oil flow-rates analysed; in this case, the interfacial stress is dominated by the high velocity of water. It can be noted also that no significant deviation can be observed in differently-inclined systems, as a further confirmation of the resemblance among Figs. 3 and 4a–c flow-pattern maps.

3. Brauner (2002) models and transition criteria: comparison to experimental data

Brauner (2002) described theoretical models developed by Brauner and co-workers to predict pressure drop and hold-up associated to the two-phase flow of an input (Q_w, Q_o) pair in a specified flow regime. Moreover, Brauner and co-workers proposed criteria to predict transition boundaries on the flow-pattern map, also reviewed in Brauner (2002).

Experimental results in terms of flow-pattern maps and associated pressure drops have been reported in Section 2 both for horizontal and slightly inclined systems, showing that no significant differences can be observed for the various inclinations. This section aims to validate theoretical and semi-empirical models by Brauner (1991), Brauner and Moalem Maron (1992), Brauner (1998), Brauner (2001) and Brauner (2002) in case of high viscosity ratio liquid–liquid flows, through comparing model predictions to the experimental data reported in Section 2.

It is worth noting that the entrance length-to-diameter ratio of the present study is $L_e/D \simeq 286$: in several works, lower L_e/D values have been considered high enough to propose interesting comparisons between experimental data and predictions of models specifically built for fully developed flow – see Appendix A. On the basis of the existent literature, the data collected in the present work have been therefore considered suitable for comparisons with predictions by the selected models.

First of all, pressure gradients obtained by the implementation of two-fluid model for core-annular flow and homogeneous no-slip model for oil-in-water dispersion will be compared to the values acquired by the differential pressure transducer on a 1.5 m pipe length.

Then, theoretical flow-pattern maps will be superimposed on experimental ones with particular attention to the regions of existence of core-annular flow and oil-in-water dispersion. A complete analysis of the stratified flow condition could not be performed due to the fewness of experimental data collected in the present tests.

3.1. Pressure drop comparison

Core-annular flow – The two-fluid model proposed by Brauner (1991), with modified shear stress closure relations Ullmann and Brauner, 2004, gives a prediction of the expected pressure drops in case of core-annular flow, once pipe inclination, fluid properties and input flow-rates are known. The model has been implemented searching by an iterative method the solution of Eq. (2), which expresses the two-fluid model combined momentum equation:

$$f(\tilde{Q}, \rho_w, \rho_o, \mu_w, \mu_o, D, \beta) = 0, \tag{2}$$

where $\tilde{Q}$ is the oil-to-water flow-rate ratio, D is the internal diameter of the pipe, β is the inclination angle (taken as positive in case of downward flow), and ρ_k and μ_k are the kth phase density and viscosity, respectively. The expression of the interfacial shear stress is based on the faster phase (oil) velocity times the difference between oil phase velocity and interfacial velocity. This closure relation, described in Ullmann and Brauner (2004), contains two adjusting parameters, F_i and c_i^0, the first one expressing the possible shear augmentation due to interfacial waviness, and the second one appearing in the expression of the interfacial velocity. In the present work, Ullmann and Brauner (2004) suggestions have been used for the choice of the values of F_i and c_i^0 parameters:

$$F_i = 1,$$
$$c_i^0 = \begin{cases} 2 & \Leftarrow \text{ laminar annular phase} \\ 1.17 & \Leftarrow \text{ turbulent annular phase} \end{cases}$$

and the resulting predictions have been compared to the experimental data.

Fig. 11 shows the comparison in case of horizontal core-annular flow; the considered two-fluid model has been also applied to the case of slightly inclined systems, as it can be observed from Fig. 12. In all the cases, the agreement between theoretical predictions and

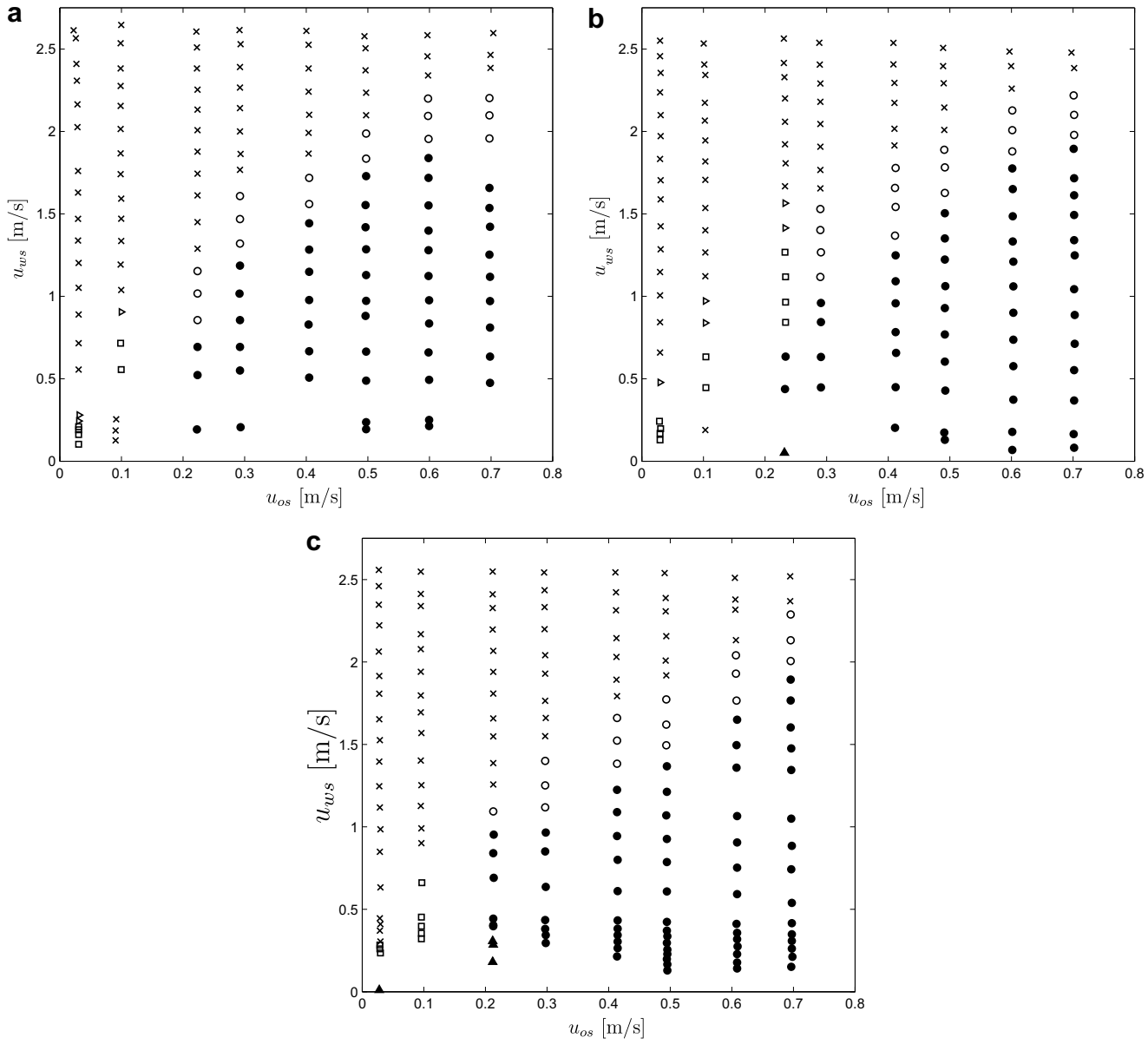

Fig. 4. Experimental flow-pattern maps. ▲ = *stratified flow*; × = *dispersion of oil in water*; • = *core-annular flow*; □ = *plug/slug flow*; ▽ = *stratified flow and dispersion of oil in water*; ○ = *core-annular flow and oil-in-water dispersion*; ▷ = *slug flow and dispersion of oil in water*. (a) 10° downward; (b) 10° upward; and (c) 15° upward.

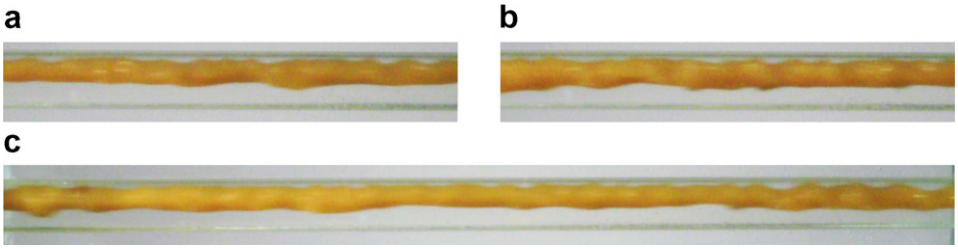

Fig. 5. Examples of observed core-annular flow ($u_{ws} \sim 1$ m/s; $u_{os} \sim 0.5$ m/s).

experimental data is fairly good, with a 85% of the compared points comprised within the ±20% agreement (dotted lines in Fig. 11) for horizontal flow, and a 70%, 80% and 64% of the compared points comprised within the ±20% agreement, for 10° downward, 10° upward and 15° upward inclined system, respectively – see Fig. 12.

It can be concluded that most of the proposed comparisons show that the theoretical model tends to underestimate frictional pressure drops associated to a core-annular flow, as argued by Brauner (2002), who recognised pipe surface roughness and core eccentricity as possible reasons for deviations.

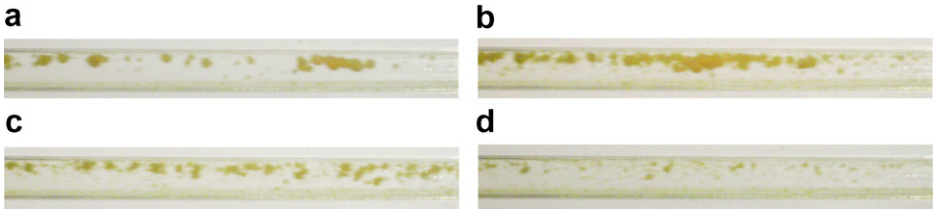

Fig. 6. Examples of observed oil-in-water dispersion ($u_{ws} = 0.7 \div 2.6$ m/s; $u_{os} = 0.03 \div 0.1$ m/s).

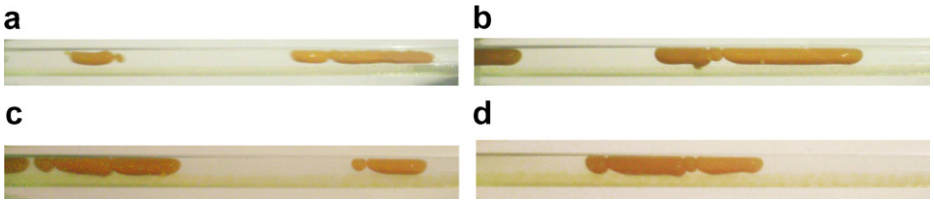

Fig. 7. Examples of oil slugs in water ($u_{ws} \sim 0.5$ m/s; $u_{os} \sim 0.1$ m/s).

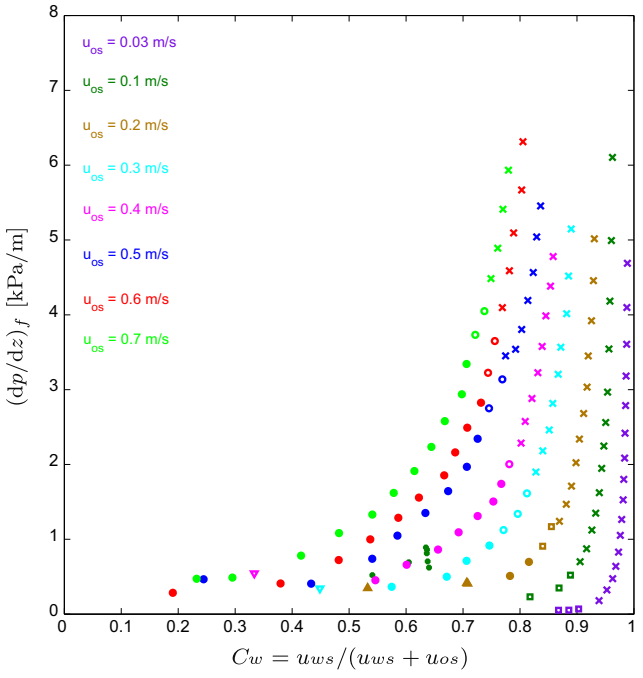

Fig. 8. Measured frictional pressure gradients as a function of input water cut (0°). ▲ = *stratified flow*; × = *dispersion of oil in water*; • = *core-annular flow*; □ = *plug/slug flow*; ▽ = *stratified flow and dispersion of oil in water*; ○ = *core-annular flow* and *oil-in-water dispersion*; ∗ = *oil film at the wall and inner dispersion of oil in water*.

Oil-in-water dispersion – The homogeneous no-slip model used by Brauner (2002) gives a prediction of the expected pressure drops in case of oil-in-water dispersion, once pipe inclination, fluid properties and input flow-rates are known. Being based on the no-slip hypothesis, the implementation of the model does not require iterations, as the hold-up can be directly computed by the knowledge of the input flow-rates:

$$\frac{Q_o}{(Q_o + Q_w)} = \frac{A_o}{(A_o + A_w)} = \epsilon_o. \tag{3}$$

As underlined in Brauner (1998), an important issue in the application of the considered model are the choice of the model for the dispersion effective viscosity μ_m. As a first try, Einstein (1906) correlation

$$\mu_m = \mu_w(1 + 2.5\epsilon_o) \tag{4}$$

can be used to model the effective viscosity. Fig. 13 shows the comparison between experimental data and predictions obtained by the model using Eq. (4) to express μ_m, in case of horizontal system. The achieved agreement is good (about 81% of the compared points within the ±20% agreement). Inclined system comparison is reported in Fig. 14. Once again, the agreement between experimental results and theoretical predictions is fairly good for all the inclinations examined (95%, 93% and 96% of the compared points within the ±20% agreement for 10° downward, 10° upward, 15° upward, respectively). It has to be kept in mind that the compared model makes use of a viscosity correlation which is suitable for dilute dispersions, and possible interfacial slip is neglected.

In view of the fact that Einstein (1906) Eq. (4) models very dilute dispersions, and that experimental observations showed the occurrence of concentrated dispersions, other models have been taken into account to represent the dispersion effective viscosity. In particular, correlations by Ball and Richmond (1980), Eq. (5), and Toda and Furuse (2006), Eq. (6), were considered:

$$\mu_m = \mu_w(1 - K\epsilon_o)^{-5/(2K)}; \tag{5}$$

$$\mu_m = \mu_w \frac{1 - 0.5\epsilon_o}{(1 - \epsilon_o)^3}. \tag{6}$$

However, the introduction of either of the two different expressions for the effective viscosity seemed not to affect significantly the homogeneous model predictions, as it can be argued from Fig. 15.

3.2. Flow-pattern map comparison

Transition criteria involving stratified, core-annular and dispersed flow regimes have been implemented and superimposed on the experimental flow-pattern maps obtained. All the examined transition criteria are reviewed in detail in Brauner (2002).

Concerning the boundary of existence of stratified flow configuration (boundary **I**), and the boundary predicting the transition from stratified flow to dispersion of oil in water and water (boundary **II**), as previously mentioned, stratified flow observations have been too few to allow comparisons, since the limitations of the water centrifugal pump did not allow to achieve sufficiently low water flow-rates to properly cover the region of existence of stratified flow-pattern. Both the lines have however been implemented, using the two-fluid model for stratified flow proposed by Brauner (2002) to evaluate water hold-up ϵ_w and, as a consequence, phase

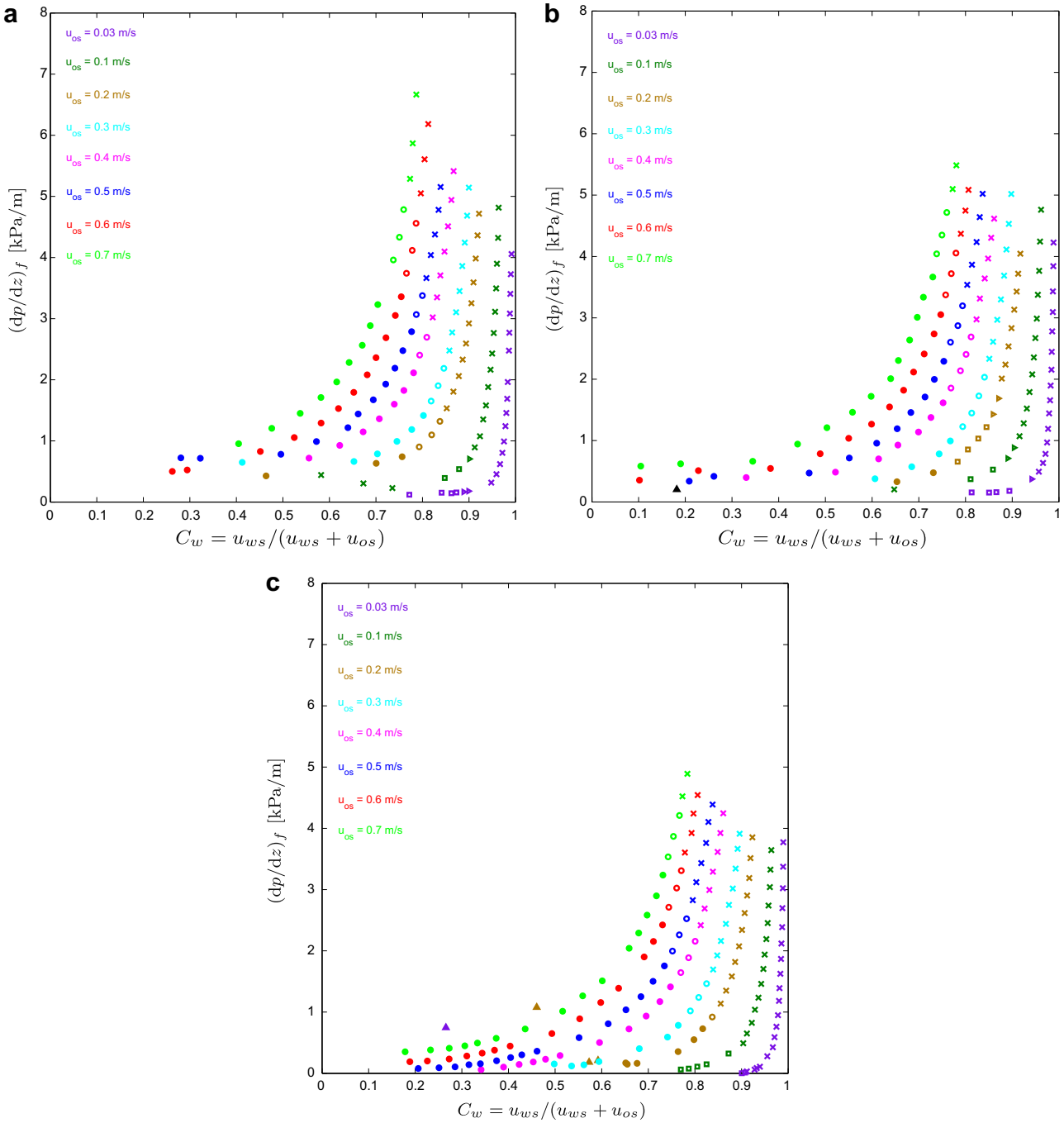

Fig. 9. Measured frictional pressure gradients as a function of input water cut. × = *dispersion of oil in water*; • = *core-annular flow*; □ = *plug/slug flow*; ○ = *core-annular flow* and *oil-in-water dispersion*; ▷ = *slug flow and dispersion of oil in water*; ▲ = *stratified flow*: (a) 10° downward; (b) 10° upward; and (c) 15° upward.

velocities U_w, U_o, areas A_w, A_o locally occupied by either of the fluids, and water layer height h, using a unitary value for the empirical waviness augmentation factor F_{iw} which can be introduced in the interfacial shear stress closure relation. Line **I** has been implemented with the following values:

$\gamma_o = 1.1,$
$\gamma_w = 1,$
$C_h = 0.$

Here, γ_k is the kth phase shape factor, which embodies the effect of the velocity profile in the kth layer. Indeed, while water layer is turbulent in the majority of the considered cases ($\gamma_w = 1$), oil phase is almost always laminar due to the oil high viscosity. For this reason Brauner (2002) suggested to slightly increase oil shape factor, γ_o. C_h is a 'sheltering coefficient' introduced by Brauner and Moalem Maron (1993) in the expression of the interfacial shear stress, to account for a 'memory' effect of the turbulent water flow. In the present analysis, C_h has been set to 0 since no correlations are currently available for liquid–liquid systems on the 'memory' effect associated to the interaction between turbulent (water) layer and a wavy interfacial boundary, though a fitting with gas–liquid data can be found in Brauner and Moalem Maron (1993).

For the implementation of line **II**, no adjustment parameters are required.

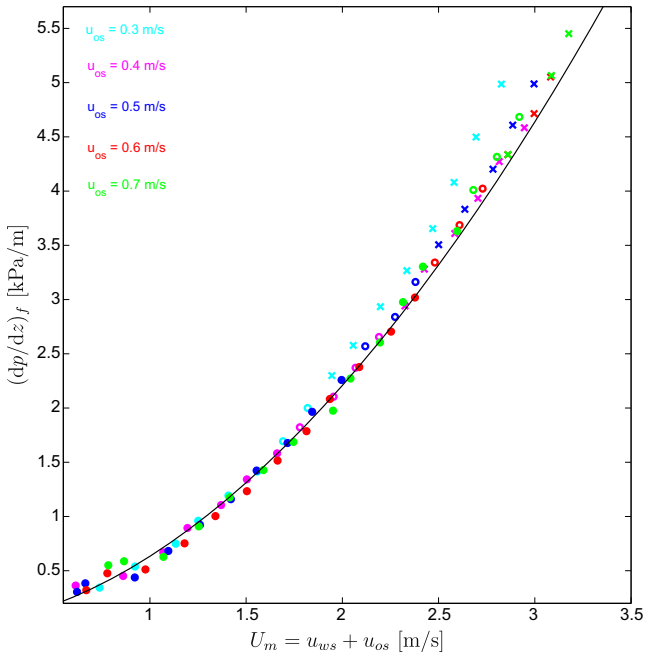

Fig. 10. Comparison between measured frictional pressure gradients at $u_{os} = 0.7$ m/s and pressure gradient associated to single phase water flow at the mixture velocity U_m. × = *dispersion of oil in water*; • = *core-annular flow*; ○ = *core-annular flow* and *oil-in-water dispersion.*

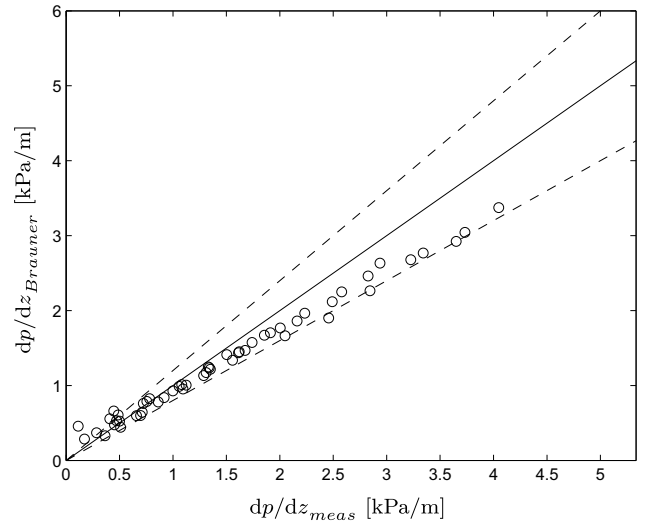

Fig. 11. Core-annular flow, 0° – Comparison between pressure gradient predictions by Brauner (2002) and measured values. The bisector is also shown (solid line).

Fig. 16 shows the predicted location of transition boundaries **I** and **II** on the flow-pattern map in case of horizontal flow.

The transition to homogeneous oil-in-water dispersion is represented by a criterion developed by Brauner (2001) and reviewed by Brauner (2002), based on the homogeneous no-slip model – Eq. (3).

The model predicts that a transition to homogeneous dispersion occurs when the maximum diameter that the drop can assume in a turbulent field, d_{max}, is smaller than the critical diameter, Eq. (8), defined as the smaller between the diameter size above which drops are deformed as an effect of interfacial tension, σ, and the diameter size above which buoyancy forces drive lighter phase drops to the upper part of the tube, promoting their coalescence:

$$d_{\text{crit}} < d_{\max}, \tag{7}$$

$$d_{\text{crit}} = \min\{d_{c\sigma}, d_{\text{cb}}\}. \tag{8}$$

The evaluation of the maximum diameter can be carried out via the so-called '*H*-model' Brauner, 2001, 2002 – proposed by Kolmogorov (1949) and Hinze (1955) for dilute dispersions, and modified by Brauner (2001) to account for dispersion concentration – provided that

$$l_k \ll d_{\max} \quad \text{and} \quad d_{\max} < 0.1D,$$

where l_k is the Kolmogorov microscale, while the second condition expresses the assumption that the length scale of energy containing eddies in a pipe of internal diameter D is larger than the maximum drop size.

In case this latter condition is not satisfied, Kubie and Gardner (1977), on the basis of previous studies by Hughmark (1971), suggested a different approach to evaluate $d_{\max}$. The resulting set of correlations, valid for diluted dispersions and also modified by Brauner (2001) to account for concentrated dispersions, is referred to as '*K*-model'.

For the scopes of the present study, the evaluation of the maximum diameter $d_{\max}$ leads to the conclusion that the *K*-model is to be used instead of *H*-model; the transition boundary obtained by the implementation of *K*-model is the **III** solid line in Fig. 17.

In view of the fact that criterion (7) predicts the map region where a homogeneous dispersion of oil drops in water would occur as a consequence of the continuous phase turbulence, and that it does not give any information on what flow regime to be expected below the boundary, it can be seen that the model well predicts the flow-pattern establishing above the boundary in all the tested flow-rate pairs. Moreover, the boundary corresponds to the experimental transition in case of the highest measured oil flow-rates.

The points indicated as 'dispersion of oil in water' situated below boundary **III**, in the map region comprised between 0.03 m/s and 0.2 m/s oil superficial velocities, are to be investigated carefully. The expected flow-pattern in this region is the so-called 'bubbly flow' – to use a nomenclature of gas–liquid field – where larger oil drops concentrate in the upper part of the tube under the effect of gravitational force. This zone is upperly bounded by oil-in-water dispersion region, and right bounded by slug/plug flow region. Recently, Ullmann and Brauner (2007) suggested a criterion to predict the transition from bubbly flow to plug flow by drop coalescence mechanism – criterion (9):

$$\epsilon_o \geqslant \epsilon_{o,\text{crit,b/s}}, \tag{9}$$

where ϵ_o is the void fraction of a train of contacting spherical bubbles with a diameter of about half the pipe diameter, while $\epsilon_{o,\text{crit,b/s}}$ is its threshold value. The resulting boundary, predicted on the basis of a critical value $\epsilon_{o,\text{crit,b/s}} = 0.1$ according to Ullmann and Brauner (2007), is reported in Fig. 18 by boundary **b/s** – which seems to predict quite well the transition to plug/slug flow.

The same considerations as those for transition boundary **III** in Fig. 17 apply also to this boundary: if we assume that on the left of the **b/s** boundary bubbly flow is observed, then a transition to elongated drop flow will occur in correspondence of the boundary. The criterion does not give information on what to expect on the left of the boundary, but it helps to locate the elongated drop region (together with boundary **IV**, which will be discussed later).

Thus, neither (7) nor (9) criterion gives prediction on what to expect in the region upperly bounded by line **III** and right bounded by line **b/s**, which is also hard to describe experimentally. Indeed, the difference between oil-in-water dispersion and bubbly flow is not easy to observe, even by 'frozen' frames captured by means of a high-speed camera. Fig. 19 shows two sequences of observations that highlight the flow regime evolution with decreasing water flow-rate for two low oil flow-rates ($u_{os} \sim 0.03$ m/s and

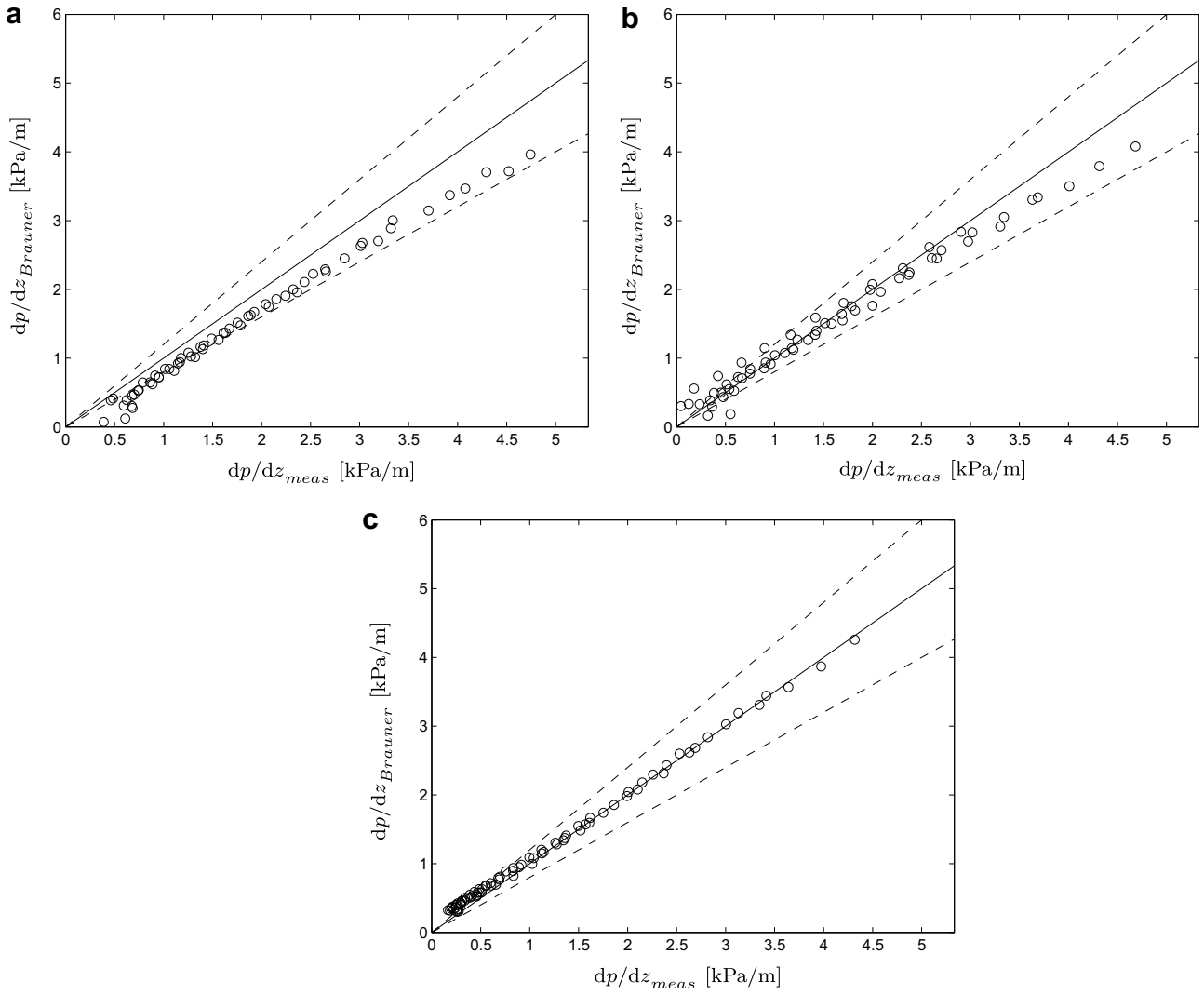

Fig. 12. Core-annular flow – Comparison between pressure gradient predictions by Brauner (2002) and measured values on a 1.5 m pipe section. The bisectors are also shown (solid lines in the figures). (a) 10° downward; (b) 10° upward; and (c) 15° upward.

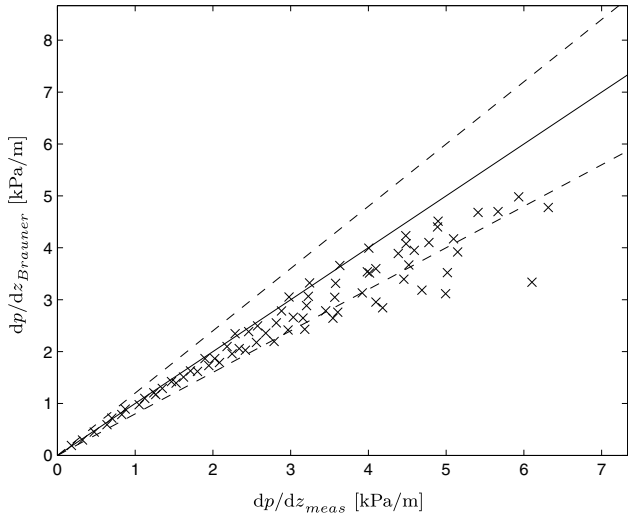

Fig. 13. Dispersion of oil in water, 0° – Comparison between pressure gradient predictions by homogeneous no-slip model and measured values on a 1.5 m pipe section. μ_m by Einstein (1906) – see Eq. (4). The bisector is also shown (solid line).

$u_{os} \sim 0.1$ m/s). From each sequence, a progressive increase in the oil drop size can be observed which pushes the oil phase to the upper part of the pipe – and this is even more evident if only the top and the bottom frames are considered in each sequence. Nevertheless, even from the pictures it is difficult to distinguish two definite zones of bubbly flow and homogeneous oil-in-water dispersion. This is the main reason why in the present study only the general definition of 'oil-in-water dispersion' has been used.

It is finally to be noted that, in those systems where the drop internal viscous force can not be neglected, Brauner (2002) suggested to apply Davies (1987) correction by multiplying the expression of the d_{max} as obtained via *H*- or *K*-model by the following term:

$$\left(1 + K_{\mu}\mu_{\mathrm{d}}\frac{u'_{\mathrm{c}}}{\sigma}\right)^{0.6}, \tag{10}$$

where μ_{d} is the viscosity of the dispersed phase, $K_{\mu} = \mathrm{O}(1)$ and u'_{c} is the characteristic turbulent fluctuating velocity in the continuous phase. The dotted **III**′ line in Fig. 17 represents the effect of (10) correction, which can be introduced in the model when the drop internal viscous force cannot be neglected: as it can be observed from

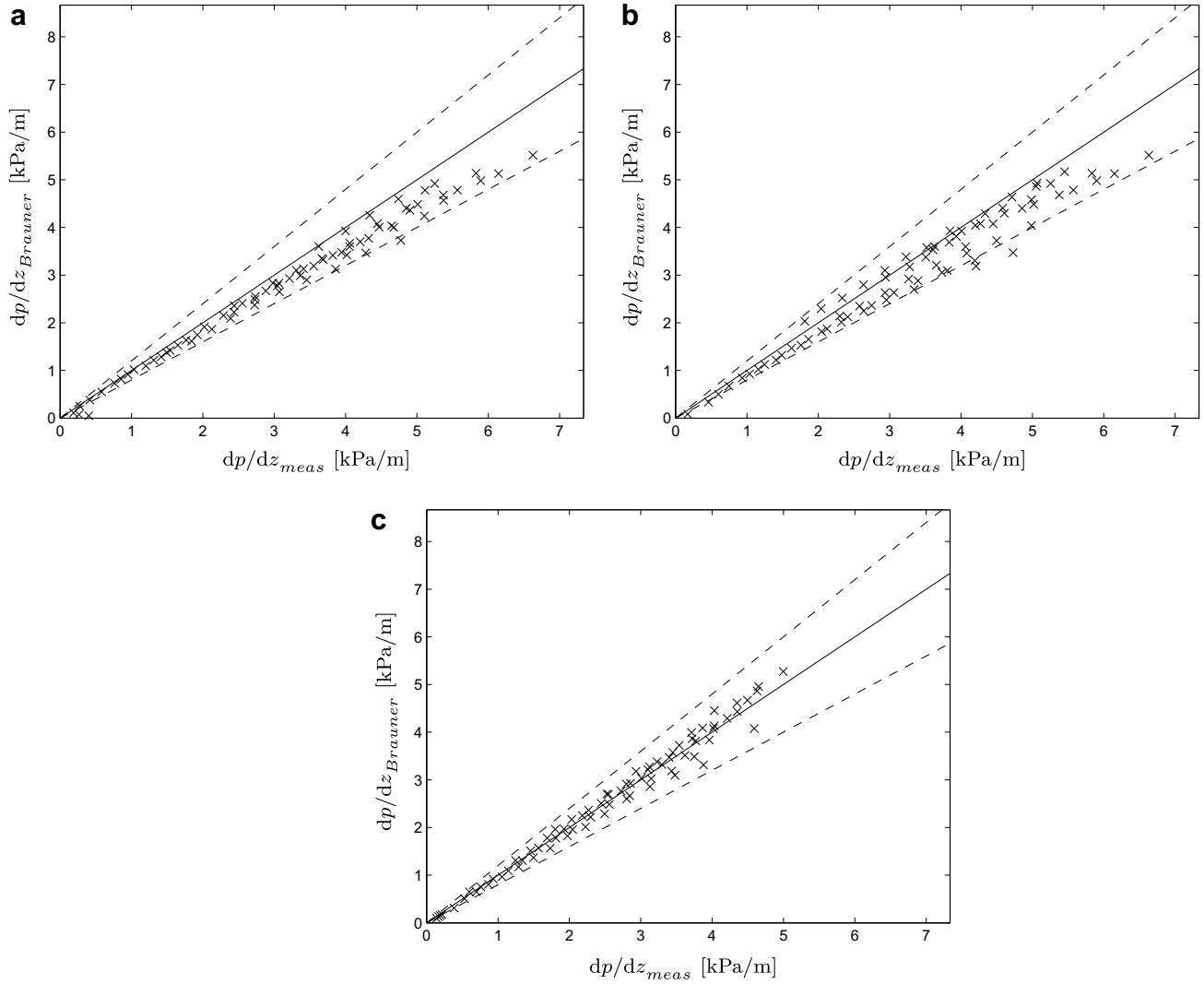

Fig. 14. Dispersion of oil in water – Comparison between pressure gradient predictions by homogeneous no-slip model and measured values on a 1.5 m pipe section. μ_m by Einstein (1906) – see Eq. (4). (a) 10° downward; (b) 10° upward; and (c) 15° upward.

the comparison, the agreement between experiments and predictions is definitely worsened by the correction.

The core rupture in core-annular flow as an effect of wave bridging by the water annulus can be predicted through the criterion proposed in Brauner and Moalem Maron (1992) and later reprised by Brauner (2002), which basically states that the core rupture occurs when

$$\epsilon_o = \epsilon_o(u_{os}, u_{ws}) \equiv \epsilon_{o,crit,IV} \,. \tag{11}$$

Once again, a model for the *in situ* hold-up is required, and the two-fluid model by Brauner (1991, 2002) was used in this work.

Brauner (2002) suggests that a critical ϵ_o value below which oil core may break up due to water wave bridging is $\epsilon_{o,crit,IV} = 0.5$. So, the criterion predicts that, starting from a core-annular flow with $\epsilon_o > 0.5$ and gradually increasing water flow-rate while keeping oil flow-rate fixed, the core breaks up when $\epsilon_o = 0.5$.

With this assumption, the result of the comparison between experimental data and predictions is far from being satisfactory, as it can be seen from the dotted line **IV′** in Fig. 20. Since $\epsilon_{o,crit,IV}$ is an empirical value depending on the system characteristics, observations were made on the 'thinnest' core that could be created with the chosen oil. It was therefore discovered that, in the hypothesis of cylindrical core, the thinnest observable core could be schematised with a approximately 1-cm-diameter cylinder, which corresponds to a 0.23 hold-up. Thus, the new critical value $\epsilon_{o,crit,IV} = 0.23$ was inserted in (11) criterion to obtain the solid **IV** line in Fig. 20. It is evident that the empirical adjustment enhanced the agreement between experimental data and predictions, which can now be considered as good. Therefore, the choice of an appropriate value for $\epsilon_{o,crit,IV}$ – for which a correlation is not available in the literature – turns to be of crucial importance in the reliability of the criterion.

The complete flow-pattern map for horizontal system is finally shown in Fig. 21. As previously mentioned, **I** boundary is located in regions of the map which are beyond the experimental water flow-rate range. As concerns inclined systems, the comparison led to the same conclusions as horizontal system. Fig. 22 shows the experimental and predicted flow-pattern maps for 10° downward, 10° upward and 15° upward systems.

4. Conclusions

A study of two-phase oil–water flow in horizontal and slightly inclined pipes has been carried out from two different viewpoints. First of all, the results of the experimental campaigns have been proposed, the most significant of which can be summarised as follows.

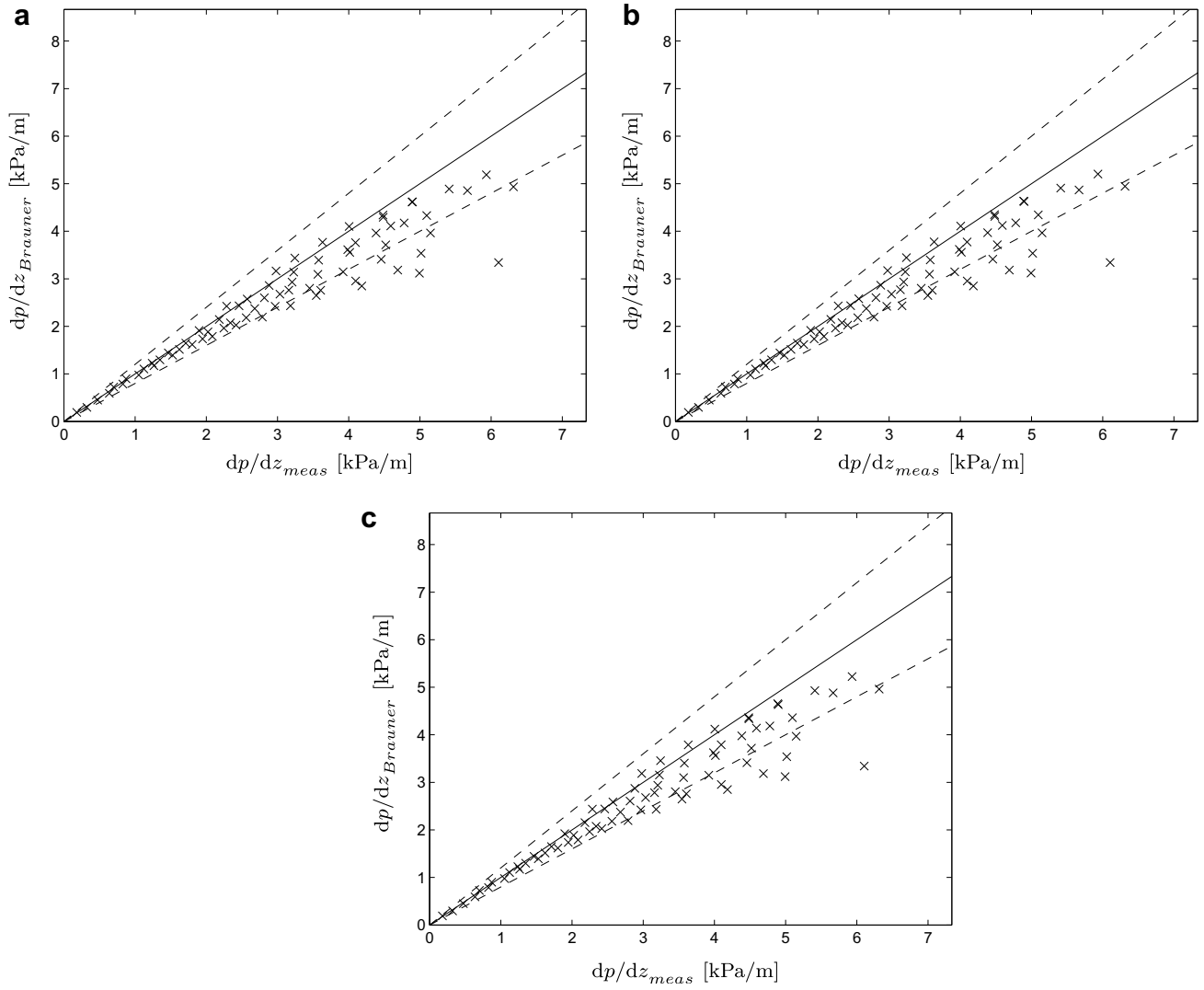

Fig. 15. Dispersion of oil in water, 0° – Comparison between pressure gradient predictions by homogeneous no-slip model and measured values: 15(a) μ_m by Ball and Richmond (1980) – see Eq. (5), with $K = 0.74$, corresponding to spheres of equal size, hexagonal close packing; 15(b) μ_m by Ball and Richmond (1980) – see Eq. (5), with $K = 0.9$, simulating the dispersion of spheres of very diverse sizes; 15(c) μ_m by Toda and Furuse (2006) – see Eq. (6).

From the analysis of experimental tests carried out on the same system with 0°, +10°, −10°, +15° inclination, no significant differences can be apparently noticed among differently inclined system, which can be related to the intermediate Eötvös number, *Eo*, characterising the system itself ($Eo \sim 1.2$).

The flow-pattern maps obtained in the described set-up show large core-annular flow and oil-in-water dispersion regions; only few occurrences of wavy stratified and none of smooth stratified flow have been observed, due to the small *Eo* characterising the system and to technological limits of the water pump; elongated oil-in-water bubbles have also been observed in small but well-defined regions of the flow-pattern maps.

Pressure drops on a 1.5 m segment of the test pipe have been measured; the results have then been compared to the values predicted by traditional formulae for the single-phase flow of water at the same mixture velocity, which seem to offer a good approximation of the problem. The theoretical studies on pressure drop and transition boundary prediction summarised in Brauner (2002) have been then taken into account, numerically implemented and applied to the set-up described in Section 2, so to make a comparison between experimental data and predictions. The evaluation of such comparative analysis leads to some significant conclusions. As concerns pressure gradient comparison, two-fluid model for core-annular flow and homogeneous no-slip model for oil-in-water dispersion Brauner, 2002 both proved to be effective tools, since the agreement between experiments and predictions is around 20% accuracy both in horizontal and in inclined system.

Contrary to the expectations, the choice of the effective viscosity expression in the implementation of oil-in-water dispersion homogeneous model does not appear to affect significantly the final prediction.

Concerning the comparison between experimental flow-pattern maps, the predicted transition boundaries involving stratified flows can not be properly evaluated due to the small number of stratified flow experimental point observed.

The boundary obtained via *K*-model well estimates the region of existence of homogeneous oil-in-water dispersed flow. In particular, the boundary corresponds to the observed transition for high oil flow-rates, while for low oil flow-rates this can not be said straightforwardly due to the difficulty in distinguishing homogeneous dispersed flow from other dispersed flow-patterns, such as bubbly flow. Furthermore, in the considered set-up, drop internal viscous force appears to be negligible in the analysis of transition to oil-in-water dispersion.

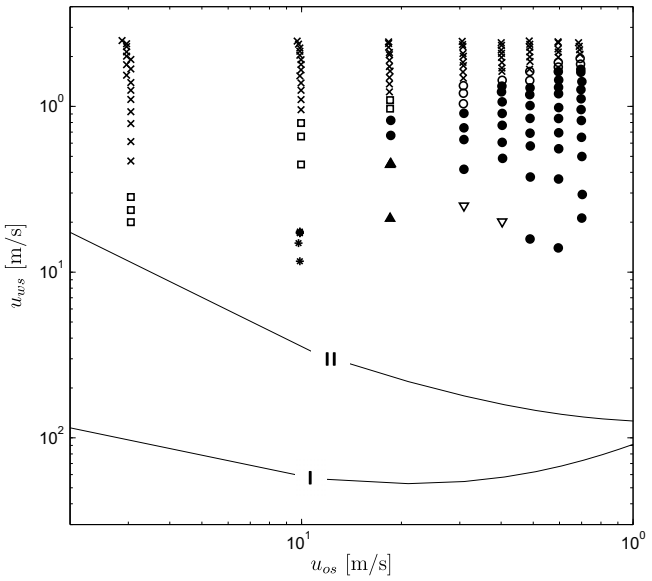

Fig. 16. 0° – Location of the predicted **I** (limit of existence of stratified configuration) and **II** (transition from stratified flow to oil-in-water dispersion and water) transition boundaries on the flow-pattern map. ▲ = *stratified flow*; × = *dispersion of oil in water*; • = *core-annular flow*; □ = *plug/slug flow*; ▽ = *stratified flow* and *dispersion of oil in water*; ○ = *core-annular flow* and *oil-in-water dispersion*; ∗ = *oil film at the wall and inner dispersion of oil in water*.

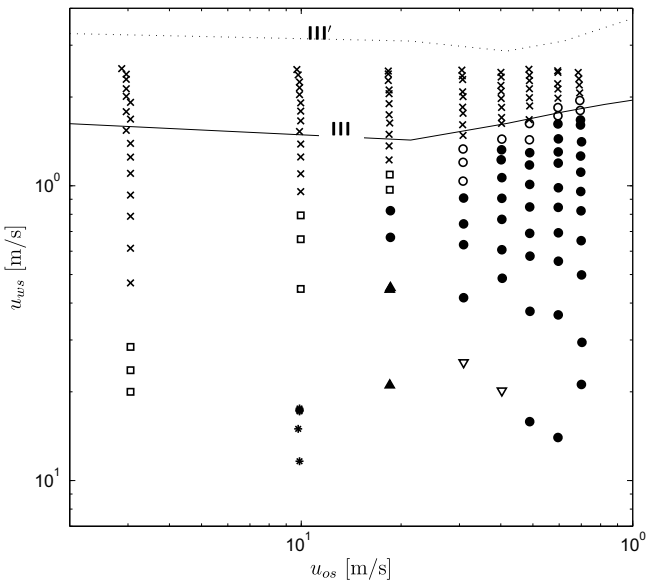

Fig. 17. 0° – Location of the predicted **III**/**III′** (in which the correction for drop internal viscous force, (10) is embedded) boundary on the flow-pattern map. ▲ = *stratified flow*; × = *dispersion of oil in water*; • = *core-annular flow*; □ = *plug/slug flow*; ▽ = *stratified flow and dispersion of oil in water*; ○ = *core-annular flow and oil-in-water dispersion*; ∗ = *oil film at the wall and inner dispersion of oil in water*.

The rupture of the oil core when in presence of a core-annular configuration is predicted to occur as a consequence of wave bridging, when water hold-up achieves a critical (maximum) value above which the oil can no longer keep its integrity. No correlation is currently available to estimate such critical value. A poor agreement is observed if the general suggestion by Brauner (2002) of 0.5 as a critical hold-up is followed; however, decreasing this value so to match the experimental observation of the thinnest observed core, the model appears to be a good tool to predict the considered transition boundary.

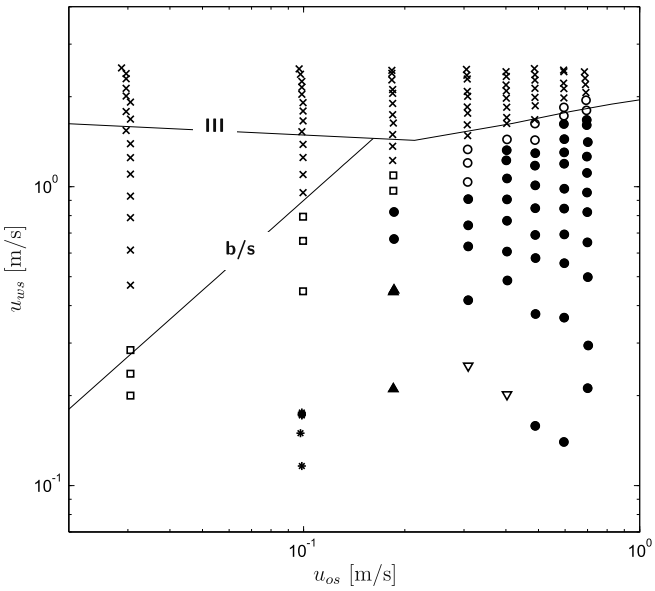

Fig. 18. 0° – Location of the predicted **III** and **b/s** (transition from bubbly to slug flow) boundary on the flow-pattern map. ▲ = *stratified flow*; × = *dispersion of oil in water*; • = *core-annular flow*; □ = *plug/slug flow*; ▽ = *stratified flow* and *dispersion of oil in water*; ○ = *core-annular flow* and *oil-in-water dispersion*; ∗ = *oil film at the wall and inner dispersion of oil in water*.

Acknowledgement

The authors would like to thank Professor Neima Brauner for the precious suggestions.

Appendix A. The choice of developing length in liquid–liquid flow experimental set-up: a brief literature summary

Finding a way to state that the flow is fully developed or not at a certain distance from the inlet is a major problem in the kind of study proposed by this paper. As a matter of fact, when performing laboratory tests, often the researchers cannot be sure they are collecting their experimental data in fully developed conditions, but neither can they be sure of the contrary. Indeed, in single-phase field several indications are available in the literature to guarantee the full development of the flow, while, to our knowledge, the topic is still open in multiphase studies.

The following problem is therefore how to validate models conceived for fully developed flow through laboratory equipment, that is to say, when a full-scale set-up is not available. Some authors studied the evolution of the wall shear stress along the pipe by measuring frictional pressure drops at several tube sections, as Çarpinlioğlu and Gündoğdu (1999) did for gas–solid flow. Often, indications are obtained by visual observations of the flow evolution along the pipe, with a purely qualitative approach. However, most of the studies are based on the fact that, being the problem of identifying a developing length not yet solved at the present time, a model validation is anyway necessary. To this aim, many authors decided to pursue an engineer approach and to use their facilities as data sources for the validation of fully-developed flow models, though being aware of a possible theoretical mismatch. Indeed, such facilities generally display a set of conditions that can be considered interesting in industrial applications. Some examples are reported in the following and summarised in A.1.

Andreini et al. (1997) used a 1000 mm length, 3 mm or 6 mm internal diameter (D) test section; the authors declared that they performed pressure measurements at the beginning of such test section, which was separated from the inlet by a 'calming section'

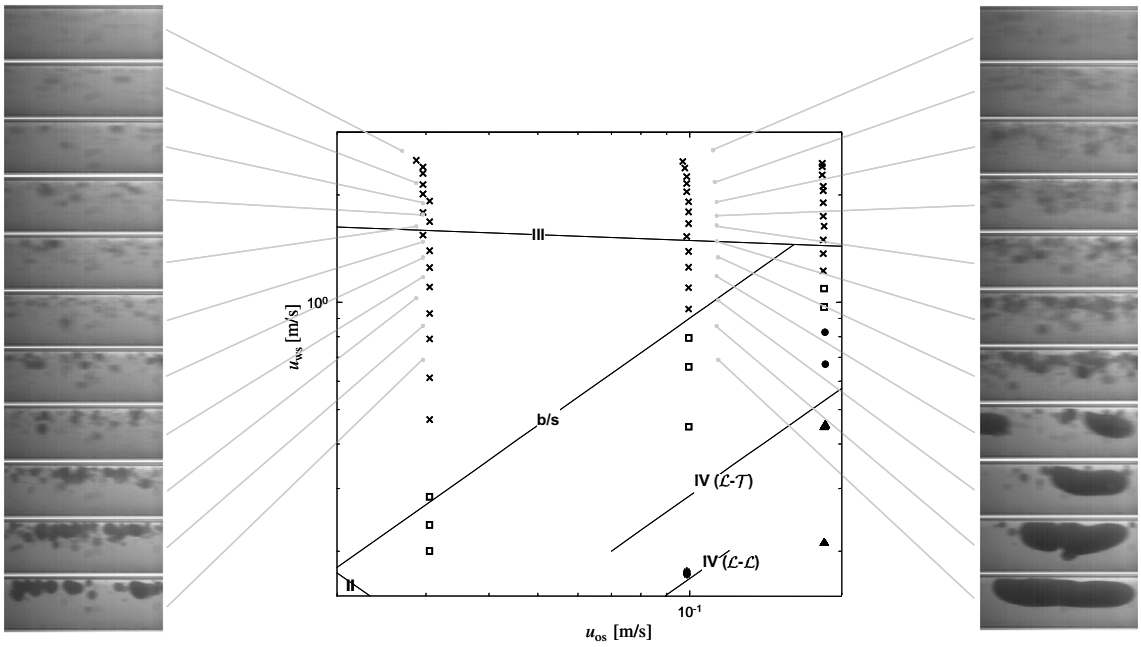

Fig. 19. 0° – Flow regime evolution at low oil flow-rates in the oil-in-water dispersion and bubbly flow zones. Pictures have been taken by means of high-speed camera, at a 300 Hz frequency. ▲ = *stratified flow*; × = *dispersion of oil in water*; • = *core-annular flow*; □ = *plug/slug flow*; ▽ = *stratified flow and dispersion of oil in water*; ○ = *core-annular flow and oil-in-water dispersion*; ∗ = *oil film at the wall and inner dispersion of oil in water.*

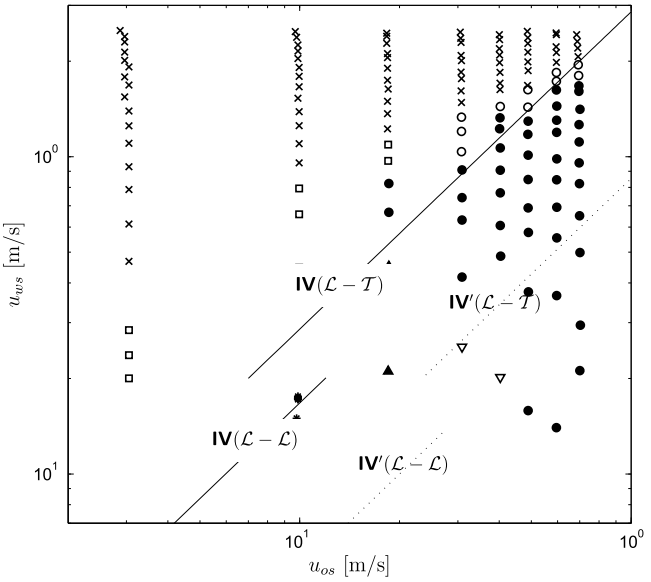

Fig. 20. 0° – Location of the predicted **IV** (core rupture in core-annular flow, $\epsilon_{o,crit,IV} = 0.23$)/**IV′** (core rupture in core-annular flow, $\epsilon_{o,crit,IV} = 0.5$) transition boundary on the flow-pattern map. ($\mathcal{L}-\mathcal{L}$) and ($\mathcal{L}-\mathcal{T}$) stand for 'laminar core - laminar annulus' and 'laminar core-laminar annulus', respectively. ▲ = *stratified flow*; × = *dispersion of oil in water*; • = *core-annular flow*; □ = *plug/slug flow*; ▽ = *stratified flow* and *dispersion of oil in water*; ○ = *core-annular flow* and *oil-in-water dispersion*; * = *oil film at the wall and inner dispersion of oil in water.*

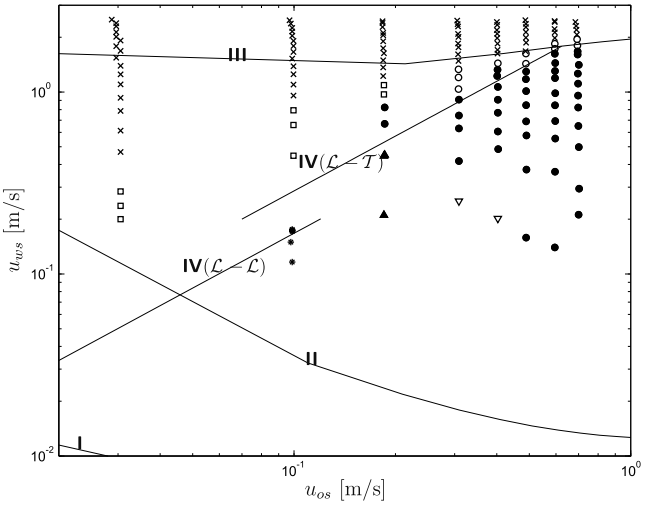

Fig. 21. 0° – Comparison between experimental flow-pattern map and transition boundaries predicted by Brauner (2002). ▲ = *stratified flow*; × = *dispersion of oil in water*; • = *core-annular flow*; □ = *plug/slug flow*; ▽ = *stratified flow* and *dispersion of oil in water*; ○ = *core-annular flow and oil-in-water dispersion*; ∗ = *oil film at the wall and inner dispersion of oil in water.*

used to eliminate entrance effects on the test section. The calming section had a length of approximately 200 times the internal diameter: the authors did not evaluate whether such values are sufficiently high to have fully developed flow, but they proposed pressure drop comparison between their experimental data and Brauner (1991) core-annular flow two-fluid model.

Also Beretta et al. (1997a,b) declared the presence of a calming section of $L_e = 600$ mm length on a pipe with $D = 3$ mm. In this case, $L_e/D = 200$, and comparisons between experimental data and model predictions were proposed concerning flow-pattern transition boundaries (Brauner, 1990) and pressure drops (Brauner, 1991).

Sunder Raj et al. (2005) stated that 'a straight developing entry section is constructed in such a fashion as to attain fully developed flow. An L/D ratio of more than 80 ensures fully developed flow before the test section'. The authors considered Trallero (1995) transition map and Brauner et al. (1996) two-fluid model for stratified flow with curved interface for hold-up prediction, and not only did they compare the model results to their own experimental data, but also used the literature data. In particular, they compared Brauner et al. (1996) model predictions to Lovick and Angeli

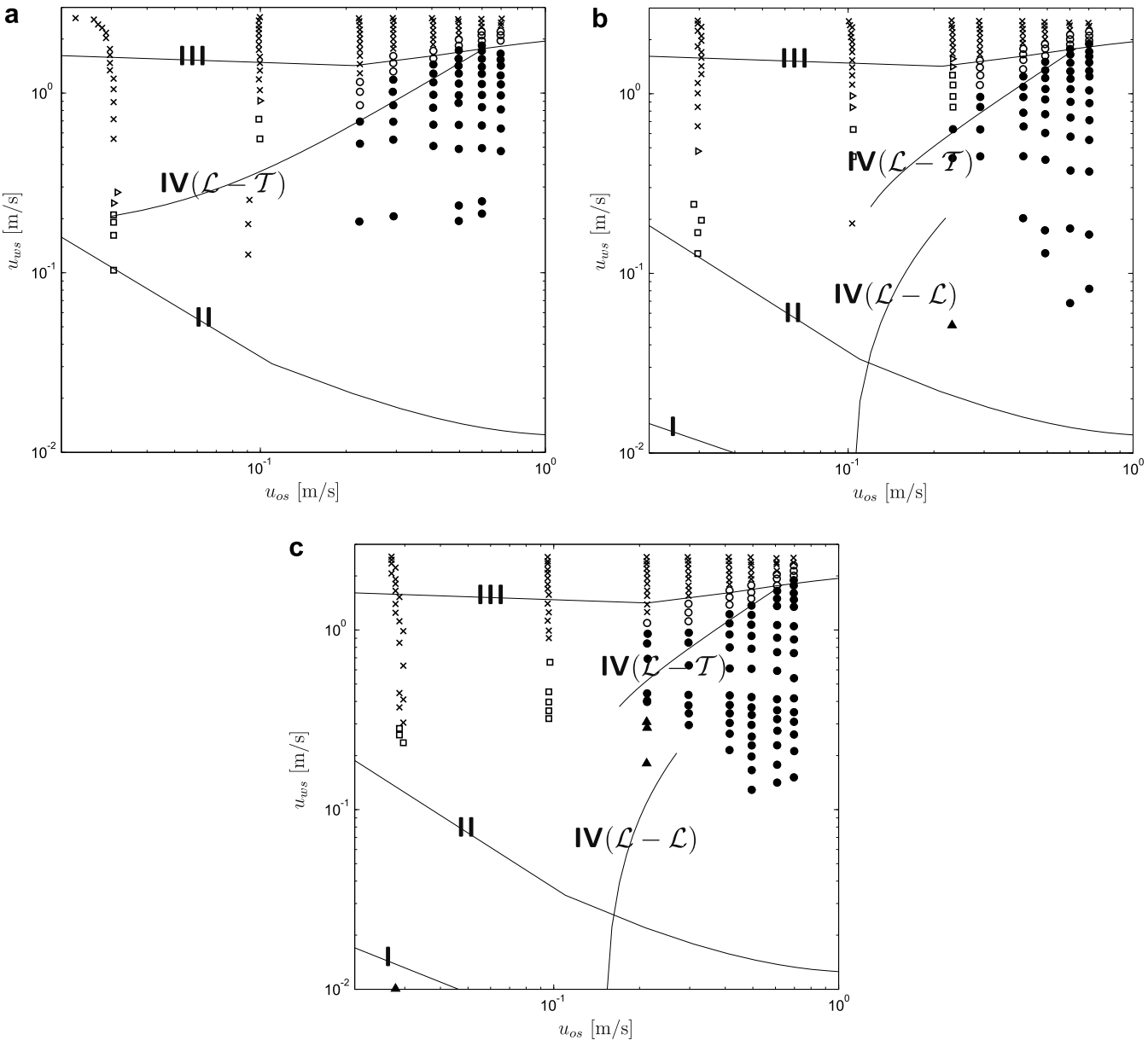

Fig. 22. Comparison between experimental and flow-pattern map and transition boundaries predicted by Brauner (2002). ▲ = *stratified flow*; × = *dispersion of oil in water*; • = *core-annular flow*; □ = *plug/slug flow*; ▽ = *stratified flow* and *dispersion of oil in water*; ○ = *core-annular flow and oil-in-water dispersion*; ▷ = *slug flow and dispersion of oil in water*. (a) 10° downward; (b) 10° upward; and (c) 15° upward.

(2004) hold-up data, obtained in a test pipe consisting of two 8-m sections of 38 mm internal diameter connected by a U-turn: this means that, even if a whole branch of the set-up is considered, the maximum length-to-diameter ratio does not exceed 211. Again, Lovick and Angeli (2004) had in their turn proposed pressure gradient comparisons with Brauner and Moalem Maron (1989) two-fluid model for stratified flow and with homogeneous model for dispersed flow.

Ullmann et al. (2004) used data by Ullmann et al. (2003) to validate new closure relations for stratified flow two-fluid model. In the latter reference, the inclining set-up is a test column consisting of three sections: an entry section and a bottom section, identical one to each other, and a middle section ($L_{\text{mid}} = 1$ m; $D_{\text{mid}} = 14.4$ mm). The entry section is 140 mm long, where the first 80 mm have a cylindrical shape ($D_{\text{e}} = 32$ mm), while the rest is shaped as cone ($D_{\text{max}} = 32$ mm; $D_{\text{min}} = 14.4$ mm). The fluids are introduced by 60-mm length tubes, still in the cylindrical part of the entry section. The authors stated that 'the establishment of fully developed conditions was verified by taking measurements of the holdup at several locations along the middle section of the pipe (30 cm downstream the entry sections). In all cases, the variations of the holdup were random and limited to the measurement error range'. Considering D_{min} in the cone part and the total middle section length, a very rough calculation gives less than 75 length-to-diameter ratio.

Brauner (2001) proposed comparisons between predicted flow-pattern transitions and experimental maps by Guzhov et al. (1973) and Trallero (1995) data. As concerns Guzhov et al. (1973), the total length-to-diameter ratio $L_{\text{TOT}}/D = 457$, and an entry section is used with $L_{\text{e}}/D = 213$. Trallero (1995) described his test section as composed of a mixing unit and upward and downward segments made up of $D = 51$ mm, $L = 1.5$ m pipes; the upward flow portion has short and long calming sections, being the first one used for sharp inclinations and the longest for nearly horizontal

Table A.1
Characteristics of experimental horizontal test tubes used for oil–water flow studies

Authors	L_e/D	$\frac{(L_e/D)_{BS}}{(L_e/D)}$
Russell et al. (1959)[a]	135	2.12
Guzhov et al. (1973)[a]	213	1.34
Malinowsky (1975)[a]	204	1.40
Laflin and Oglesby (1976)[a]	480	0.60
Oglesby (1979)[a]	275	1.04
Cox (1985)[a]	102	2.80
Scott (1985)[a]	102	2.80
Herm-Stapelberg and Mewes (1990)[a]	120	2.38
Trallero (1995)	92	3.11
	152	1.88
Valle and Kvandal (1995)[a]	176	1.63
Andreini et al. (1997)	200	1.43
Beretta et al. (1997a,b)	200	1.43
Nädler and Mewes (1997)[a]	226	1.27
Ullmann et al. (2003)	$\leqslant 75$	$\geqslant 3.81$
Lovick and Angeli (2004)	$\leqslant 211$	$\geqslant 1.36$
Sunder Raj et al. (2005)	80	3.58

Column on the right displays the value of the ratio between the entry length-to-diameter ratio in Brescia set-up $(L_e/D)_{BS}$ and the value of L_e/D as reported in the corresponding reference.

[a] References are taken from Trallero (1995).

flow: the declared length-to-diameter ratios are 92 and 152, respectively.

Coming to the present experimental facility, the test tube consists of six 1.5 m segments with an internal diameter $D = 21$ mm. Fig. 1 shows that the differential pressure transducer plugs are placed at the ends of the fifth tube, where also the observation box is. That is to say, a 6 m length separates the inlet device from the test segment, which is in its turn separated from the outlet by a 1.5 m length. In the present case, the entry section is therefore characterised by $L_e/D = 6/0.021 \sim 286$, which is a higher value if compared to the above references.

Trallero (1995) summarised the research published for oil–water flow in case of horizontal pipes. He noticed that for these studies the entrance length usually does not exceed $200D$. Looking at Table A.1, in which a direct comparison is possible with Brescia experimental facility, it can be observed that the set-up used for the present study is characterised by the second highest L_e/D (only in Laflin and Oglesby (1976) the value is higher than in Brescia set-up).

To conclude, the problem of knowing where the two-phase flow is fully developed exists and, to our knowledge, no straightforward solutions are currently available in the literature. However, most of authors who proposed comparisons between their experimental data and models conceived for fully developed flow pursued an engineer approach, based on the consideration that such data were collected in a set of conditions that could be thought interesting from a practical point of view.

In the present paper, the same approach was chosen in attempting to validate models through experimental data.

References

Andreini, P.A., De Greeff, P., Galbiati, L., Kuhlwetter, A., Sotgia, G., 1997. Oil–water flow in small diameter tubes. In: Proceedings of the International Symposium on Liquid–liquid Two-phase Flow and Transport Phenomena, Antalya, Turkey.

Angeli, P., Hewitt, G.F., 1998. Pressure gradient in horizontal liquid–liquid flows. Int. J. Multiphas. Flow 24, 1183–1203.

Arirachakaran, S., Oglesby, K.D., Malinowsky, M.S., Shoham, O., Brill, J.P., 1989. An analysis of oil/water flow phenomena in horizontal pipes. SPE Proc. Prod. Oper. S. SPE18836, 155–167.

Arney, M.S., Bai, R., Guevara, E., Joseph, D.D., 1992. Lubricated pipelining: stability of core-annular flow Part 5. Experimental and comparison with theory. J. Fluid Mech. 240, 97–132.

Ball, R., Richmond, P., 1980. Dynamics of colloidal dispersions. J. Phys. Chem. Liq. 9, 99–116.

Bannwart, A.C., 1998. Wavespeed and volumetric fraction in core annular flow. Int. J. Multiphas. Flow 24, 961–974.

Beretta, A., Ferrari, P., Galbiati, L., Andreini, P.A., 1997a. Horizontal oil–water flow in small diameter tubes. Flow patterns. Int. Commun. Heat Mass 24, 223–229.

Beretta, A., Ferrari, P., Galbiati, L., Andreini, P.A., 1997b. Horizontal oil–water flow in small diameter tubes. Pressure drop. Int. Commun. Heat Mass 24, 231–239.

Brauner, N., 1990. On the relations between two-phase flow under reduced gravity and earth experiment. Int. Commun. Heat Mass Transfer 17, 271.

Brauner, N., 1991. Two-phase liquid–liquid annular flow. Int. J. Multiphas. Flow 17, 59–76.

Brauner, N., 1998. Liquid–liquid two-phase flow. HEDU – Heat Exchanger Design Handbook. Begell House, New York (Chapter 2.3.5).

Brauner, N., 2001. The prediction of dispersed flows boundaries in liquid–liquid and gas–liquid systems. Int. J. Multiphas. Flow 27, 885–910.

Brauner, N., 2002. Liquid–liquid two-phase flow systems. In: Bertola, V. (Ed.), Modeling and Control of Two-phase Flow Phenomena. CISM Center, Udine, Italy.

Brauner, N., Moalem Maron, D., 1989. Two phase liquid–liquid stratified flow. PhysicoChem. Hydrodynam. 11, 487–506.

Brauner, N., Moalem Maron, D., 1992. Flow-pattern transitions in two-phase liquid–liquid flow in horizontal tubes. Int. J. Multiphas. Flow 18, 123–140.

Brauner, N., Moalem Maron, D., 1993. The role of interfacial shear modelling in predicting the stability of stratified two-phase flow. Chem. Eng. Sci. 8, 2867–2879.

Brauner, N., Rovinsky, J., Moalem Maron, D., 1996. Determination of the interface curvature in stratified two-phase systems by energy considerations. Int. J. Multiphas. Flow 22, 1167–1185.

Çarpinlioğlu, M.Ö., Gündoğdu, M.Y., 1999. Effect of particle size and loading on development region in two-phase flows. Tr. J. Eng. Env. Sci. 23, 27–37.

Charles, M.E., Govier, G.W., Hodgson, G.W., 1961. The horizontal pipeline flow of equal density oil–water mixture. Can. J. Chem. Eng. 39, 27–36.

Cox, A.L., 1985. A study of horizontal and downhill two-phase oil–water flow. M.Sc. Thesis, The University of Texas.

Davies, J.T., 1987. A physical interpretation of drop sizes in homogeneous agitated viscous oils. Chem. Eng. Sci. 42, 1671–1676.

Einstein, A., 1906. Eine neue Bestimmung der Molekldimensionen. Ann. Phys. 19, 289–306.

Grassi, B., Poesio, P., Piana, E., Lezzi, A.M., Beretta, G.P., 2006. Influence of inlet conditions on flow patterns in oil–water flows in horizontal tubes at intermediate Eötvös number. In: 6th Euromech Fluid Mechanics Conference Stockholm, Sweden.

Guzhov, A.I., Grishin, A.D., Medredev, V.F., Medredeva, O.P., 1973. Emulsion formation during the flow of two immiscible liquids. Neft. Choz. 8, 58–61.

Guzhov, A.I., Medvedev, O.P., 1971. Pressure losses in flow of two mutually immiscible liquids. Int. Chem. Eng. 11, 104–106.

Hadžiabdić, M., Oliemans, R.V.A., 2007. Parametric study of a model for determining the liquid flow-rates from the pressure drop and water hold-up in oil–water flows. Int. J. Multiphas. Flow 33, 1365–1394.

Hasson, D., Mann, U., Nir, A., 1970. Annular flow of two immiscible liquids I. Mechanisms. Can. J. Chem. Eng. 48, 514–520.

Herm-Stapelberg, H., Mewes, D., 1990. The flow of two immiscible liquids and air in a horizontal pipe. In: Winter Annual Meeting of the ASME, pp. 89–96.

Hinze, J.O., 1955. Fundamentals of the hydrodynamic mechanism of splitting in dispersion processes. AIChE J. 1, 289–295.

Hu, B., Matar, O.K., Hewitt, G.F., Angeli, P., 2006. Population balance modelling of phase inversion in liquid–liquid pipeline flows. Chem. Eng. Sci. 61, 4994–4997.

Hughmark, G.A., 1971. Drop breakup in turbulent pipe flow. AIChE J. 17, 1000.

Ioannou, K., Nydal, O.J., Angeli, P., 2005. Phase inversion in dispersed liquid–liquid flows. Exp. Therm. Fluid Sci. 29, 331–339.

Kolmogorov, A.N., 1949. On the breaking of drops in turbulent flow. Dokl. Akad. Nauk. SSSR 66, 825–828.

Kubie, J., Gardner, G.C., 1977. Drop sizes and drop dispersion in straight horizontal tubes and in helical coils. Chem. Eng. Sci. 32, 195–202.

Laflin, G.C., Oglesby, K.D., 1976. An experimental study on the effects of flow rate, water fraction and gas–liquid ratio on air–oil–water flow in horizontal pipes. B.S. Thesis, The University of Tulsa.

Lovick, J., Angeli, P., 2004. Experimental studies on the dual continuous flow pattern in oil–water flows. Int. J. Multiphas. Flow 30, 139–157.

Malinowsky, M.S., 1975. An experimental study on oil–water and air–oil–water flowing mixtures in horizontal pipes. MS Thesis, University of Tulsa.

Nädler, M., Mewes, D., 1997. Flow induced emulsification in the flow of two immiscible liquids in horizontal pipes. Int. J. Multiphas. Flow 23, 55–68.

Oglesby, K.D., 1979. An experimental study on the effects of viscosity, mixture velocity, and water fraction on horizontal oil–water flow. M.Sc. Thesis, The University of Tulsa.

Piela, K., Delfos, R., Ooms, G., Westerweel, J., Oliemans, R.V.A., Mudde, R.F., 2006. Experimental investigation of phase inversion in an oil–water flow through a horizontal pipe loop. Int. J. Multiphas. Flow 32, 1087–1099.

Poesio, P., Strazza, D., Grassi, B., Margarone, M., 2007. Statistical measurements in horizontal and slightly inclined oil-in-water slug flow. In: Proceedings of the International Conference on Multiphase Flow. Leipzig, Germany.

Rodriguez, O.M.H., Oliemans, R.V.A., 2006. Experimental study on oil–water flow in horizontal and slightly inclined pipes. Int. J. Multiphas. Flow 32, 323–343.

Russell, T.W.F., Charles, M.E., 1959. The effect of the less viscous liquid in the laminar flow of two immiscible liquids. Can. J. Chem. Eng. 37, 18–34.
Russell, T.W.F., Hodgson, G.W., Govier, G.W., 1959. Horizontal pipeline flow of mixtures of oil and water. Can. J. Chem. Eng. 37, 9–17.
Scott, G.M., 1985. A study of two-phase liquid–liquid flow at variable inclinations. M.Sc. Thesis, The University of Texas.
Sotgia, G., Tartarini, P., 2004. The flow of oil–water mixtures in horizontal pipes. State of the art and recent developments on pressure drop reductions and flow regime transitions. In: Proceedings of the Third International Symposium on Two-Phase Flow Modelling and Experimentation, Pisa, Italy.
Strazza, D., Grassi, B., Poesio, P., 2007. Core-annular flow in slightly inclined flows: existence and pressure drops. In: Proceedings of the International Conference on Multiphase Flow, Leipzig, Germany.
Sunder Raj, T., Chakrabarti, D.P., Das, G., 2005. Liquid–liquid stratified flow through horizontal conduits. Chem. Eng. Technol. 28, 899–907.
Toda, K., Furuse, H., 2006. Extension of Einstein's viscosity equation to that for concentrated dispersions of solutes and particles. J. Biosci. Bioeng. 102, 524–528.
Trallero, J.L., 1995. Oil–water flow patterns in horizontal pipes. PhD Thesis, The University of Tulsa.
Ullmann, A., Brauner, N., 2004. Closure relations for the shear stresses in two-fluid models for core-annular flow. Multiphas. Sci. Technol. 16, 355–387.
Ullmann, A., Brauner, N., 2007. The prediction of flow pattern maps in mini channels. Multiphas. Sci. Technol. 19, 49–73.
Ullmann, A., Goldstein, A., Zamir, M., Brauner, N., 2004. Closure relations for the shear stresses in two-fluid models for laminar stratified flow. Int. J. Multiphas. Flow 30, 877–900.
Ullmann, A., Zamir, M., Ludmer, Z., Brauner, N., 2003. Stratified laminar countercurrent flow of two liquid phases in inclined tubes. Int. J. Multiphas. Flow 29, 1583–1604.
Valle, A., Kvandal, H., 1995. Pressure drop and dispersion characteristics of separated oil/water flow. In: Proceedings of the First International Symposium on Two-Phase Flow Modelling Experimentation, Rome, Italy.
Zhao, Y.C., Chen, G.W., Yuan, Q., 2006. Liquid–liquid two-phase flow patterns in a rectangular microchannel. AIChE J. 52, 4052–4060.